5d Orbital and Electronic Localization in Rare Earth Diiodides and Pr_2X_5 (X = Br, I)

Yunchao Tian and Timothy Hughbanks*

Department of Chemistry, Texas A&M University, College Station, Texas 77843-3255

Received June 4, 1992

An analysis of the origin of the valence and conduction band gaps and bandwidths for the LnI_2 (Ln = La, Ce, Pr, Gd) compounds is presented. The PrI_2 system is analyzed in detail with a focus on the 3-center bonding present in these compounds, as was found for the isostructural MoS_2 system. Despite the long Ln–Ln distances found in these compounds, appreciable band gaps arise that are traceable to the splitting between the bonding and antibonding orbitals of the 3-center bond systems. We argue that the narrowness of the valence band is not due to the weakness of the metal–metal interactions. Comparison with the Pr_2X_5 (X = Br, I) systems treated by Meyer and Hoffmann shows the close analogies between the electronic structure of these compounds and the LnI_2 materials. A hybridization scheme for the low-lying d levels of trigonal prismatic centers clearly reveals these relationships. Since the Pr_2X_5 compounds are magnetically ordered with localized 5d electrons, questions about the properties of the LnI_2 compounds are raised.

Introduction

The localization of 4f electrons in the "cores" of the lanthanide elements, regardless of whether they are combined in their elemental forms or in compounds, is the normal state of affairs. Since the radial extent of the 4f orbitals is so limited, 4f electrons interact much more strongly among themselves, via electronic repulsion, than with surrounding atoms in the environment of the lanthanide center. In contrast, the remaining valence orbitals (5d, 6s, 6p) of the lanthanides strongly mix with neighboring atom orbitals to form bonds. Thus, when dealing with reduced rare earth compounds (as, for example, GdI_2, DyI_2, Gd_2Cl_3, Gd_4I_5C, SmS, GdS, EuO, etc.), one can usually perform the following categorization: (i) The rare earth element is "divalent", and extra electrons are taken up in the 4f core, as for EuO. (ii) The rare earth element is "trivalent", and extra electrons are to be found in a conduction band, often of unspecified character, but are assumed to have largely metal 5d character, as in GdS or Gd_4I_5C. (iii) The rare earth element is occasionally "mixed-valent", and the extra electrons' character fluctuates between the 4f cores and the valence 5d orbitals, as for SmS when under a modest pressure.[1]

Along with these categories come expectations for physical properties. Divalent EuO is an electrical insulator, since there are no itinerant electrons outside the Eu($4f^7$) core to fill a conduction band. GdS and Gd_4I_5C are metallic, since they do have extra electrons outside the Gd($4f^7$) cores that fill largely Gd localized conduction band orbitals.[2,3] SmS exhibits, among other fascinating properties, an insulator-to-metal transition with increased pressure that is correlated with a divalent-to-trivalent change in electronic structure.[1] There are other surprises—Gd_2Cl_3 is semiconducting despite the fact that Gd is trivalent and there are 1.5 surplus electrons per metal center devoted to Gd–Gd bonding.[4-6] We have recently demonstrated how the Gd 5d electrons in this compound can localize into both 2-center and 4-center Gd–Gd bonding orbitals that do *not* spread over the length of the continuous Gd–Gd bonded chains found in the structure.[7]

The localization of electrons in Gd_2Cl_3, while surprising, is actually of the same character as the localization of electrons in more familiar covalent semiconductors and insulators. Electrons are paired in valence band orbitals, and there is a valence-conduction band gap. Elemental silicon is a distant analog! The valence band of silicon may be crudely understood as arising from the interaction between the *localized* Si–Si σ orbitals that bridge the sp^3-hybridized silicon centers. Likewise, the conduction band in silicon arises from the spreading of interacting Si–Si σ^* orbitals.[8] Similarly, in Gd_2Cl_3 the valence band is built up from modestly interacting *localized* orbitals.[7]

The materials Pr_2X_5 (X = Br, I) are also semiconducting, but the localization here is of a different character. These materials have a surprising magnetic *insulating* ground state[9] and as demonstrated by Meyer and Hoffmann (see below), have a half-filled 5d valence band in which electrons are localized.[10] In the present paper we will examine the rare earth diiodides and the Pr_2X_5 compounds, in order to gain a better understanding of the circumstances under which 5d electron localization might occur. If we do not give definitive answers to all the questions raised, then we hope to cast the problems in a useful form.

Trigonal Prismatic Structures: LnI_2

Before we turn to an investigation of specific compounds, let us reexamine the d orbital splitting induced in metals in a trigonal prismatic environment. We will be brief since this follows many previous treatments, including that recently given by Meyer and Hoffmann, though our approach differs in some important aspects.[10] Figure 1 shows a Walsh diagram for the d levels of PrI_6 trigonal prism as a function of the c/a ratio of the prism (i.e., the ratio of the I–I distances parallel to the 3-fold axis, c, to those perpendicular, a). At one extreme on the diagram is the geometry ($c/a = \sqrt{2/3}$) one obtains for a prism obtained by rotating one I_3 face of an octahedron by 60° relative to the opposite I_3 face, keeping the Pr at the center. At this point the I ligands reside in the node of the d_{z^2} orbital, and this a_1' symmetry level should

(1) Varma, C. M. *Rev. Mod. Phys.* **1976**, *48*, 219.
(2) Simon, A. *J. Solid State Chem.* **1985**, *57*, 2.
(3) Kauzlarich, S. M.; Hughbanks, T.; Corbett, J. D.; Klavins, P.; Shelton, R. N. *Inorg. Chem.* **1988**, *27*, 1791.
(4) Ebbinghaus, G.; Simon, A.; Griffith, A. *Z. Naturforsch.* **1982**, *A37*, 564.
(5) Bauhofer, W.; Simon, A. *Z. Naturforsch.* **1982**, 568.
(6) Kremer, R. K.; Mattausch, H.; Simon, A.; Steuernagel, S.; Smith, M. E. *J. Solid State Chem.* **1992**, *96*, 237.
(7) Yee, K. A.; Hughbanks, T. *Inorg. Chem.* **1992**, *31*, 1620.
(8) Harrison, W. A. *Electronic Structure and Properties of Solids*; Freeman: San Francisco, CA, 1980.
(9) Krämer, K.; Meyer, G.; Fischer, P.; Hewat, A. W.; Güdel, H. U. *J. Solid State Chem.* **1991**, *95*, 1.
(10) Meyer, H.-J.; Hoffmann, R. *J. Solid State Chem.* **1991**, *95*, 14.

0020-1669/93/1332-0400$04.00/0

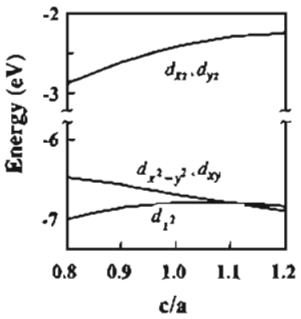

Figure 1. d level Walsh diagram for a PrI_6 trigonal prism, calculated by using fixed Pr–I bond lengths and plotted vs the c/a ratio of the prism. The z-axis coincides with the C_3 axis of the trigonal prism.

be nonbonding (at least with respect to Pr–I σ interactions). The e′ orbitals $\{d_{x^2-y^2}, d_{xy}\}$ are pushed up to some extent by Pr–I antibonding interactions, and the e″ orbitals $\{d_{xz}, d_{yz}\}$ are strongly antibonding.

The "ideal" geometry described above is unlikely for realistic trigonal prismatic coordination because ligand–ligand contacts between triangular faces are too severely crowded. It is more common to find c/a ratios nearer to 1, for which the d_{z^2}–$\{d_{x^2-y^2}, d_{xy}\}$ orbital splitting becomes small as the ligands move out of the d_{z^2} orbital node and further out of the xy plane where there is maximal overlap with the $\{d_{x^2-y^2}, d_{xy}\}$ orbitals. This is an important point that is sometimes not appreciated in considering materials where trigonal prismatic metal coordination is involved. It implies that if there are perturbations to these levels which are much greater in magnitude than the d_{z^2}–$\{d_{x^2-y^2}, d_{xy}\}$ orbital splitting, then this splitting can be neglected when we treat the effects of such perturbations. Specifically, if we wish to consider the interaction of the central metal with atoms that cap the square faces of the prism (**1**), then the strength of that interaction will be much more important than the small gap that separates the d_{z^2} and $\{d_{x^2-y^2}, d_{xy}\}$ orbitals.

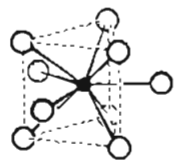

1

A method that we previously introduced in accounting for interactions through the square faces of a trigonal prism involves the construction of three equivalent hybrids from the d_{z^2} and $\{d_{x^2-y^2}, d_{xy}\}$ orbitals:[11]

$$\sigma_1 = \frac{-1}{\sqrt{3}}d_{z^2} + \frac{\sqrt{2}}{\sqrt{3}}d_{x^2-y^2}$$

$$\sigma_2 = \frac{-1}{\sqrt{3}}d_{z^2} - \frac{1}{\sqrt{6}}d_{x^2-y^2} - \frac{1}{\sqrt{2}}d_{xy} \qquad (1)$$

$$\sigma_3 = \frac{-1}{\sqrt{3}}d_{z^2} - \frac{1}{\sqrt{6}}d_{x^2-y^2} + \frac{1}{\sqrt{2}}d_{xy}$$

These are indicated schematically in **2**. Each of these orbitals is well directed for σ overlap with a ligand on one of the square faces. There is only a small residual overlap of these hybrids with orbitals that reside on faces for which the hybrids are "not intended". (If we place a σ-bonding ligand orbital, χ, over the face normal to the x axis, the following overlap ratios are obtained: $|\langle\sigma_2|\chi\rangle/\langle\sigma_1|\chi\rangle| = |\langle\sigma_3|\chi\rangle/\langle\sigma_1|\chi\rangle| = 0.065$.) Finally, we see that the set of equivalent d "hybrids" can be formed from a nearly degenerate set of basis orbitals and interact with external "capping" orbitals in a nearly independent fashion.

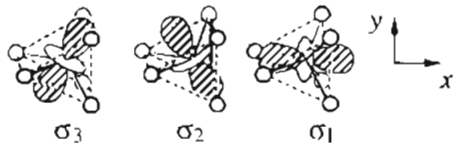

2

Now let us piece structures together; we will refer to the set of orbitals σ_1, σ_2, and σ_3 in order to interpret the results of our band structure calculations. The layered diiodides, LnI_2 (Ln = La, Ce, Pr, Gd), all adopt structures in which metal centers have trigonal prismatic coordination.[12,13] We have recently treated this problem with reference to MoS_2 and other layered dichalcogenides, so our discussion can be brief. In Figure 2, we see the structure of the trigonal prismatic layer, accompanied by an illustration showing the overlap of hybrids from three adjacent trigonal prisms. Since each trigonal prism is surrounded by three identical sites, each hybrid of every trigonal prismatic center becomes involved in a 3-center bond. Naturally, the hybrids need not combine to form bonding combinations—a degenerate set of antibonding combinations may be constructed in each triangle as well. In all of this, the extent to which the hybrids interact *independently* is important because the 3-center bonding orbitals (of a_1' symmetry) and antibonding orbitals (of e′ symmetry) should then give rise to narrow bands. Also, the band gap between the 3-center bonding and antibonding band is determined by the size of the metal–metal overlap.

In a manner exactly analogous to our treatment of MoS_2, we can construct local (Wannier) orbitals for both the valence and conduction bands for the LnI_2 systems to confirm the qualitative analysis we have laid out above.[11] Figure 3 shows a density of states (DOS) diagram calculated for a single PrI_2 layer[13] and the projected DOS for the bands that are symmetric with respect to reflection in the layer plane. For the energy range plotted, the

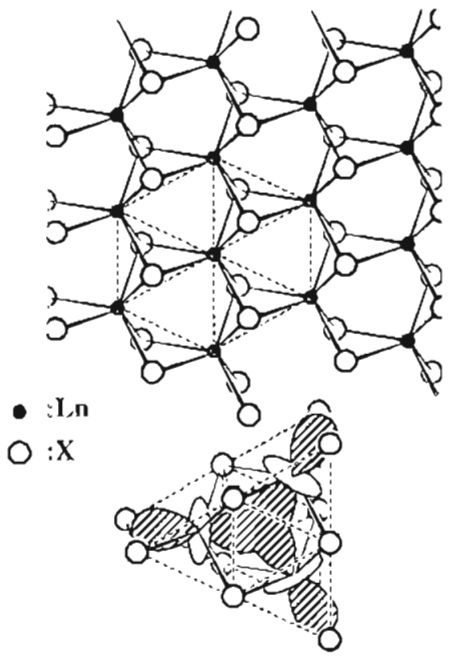

Figure 2. One layer of the LnX_2 structure, where the dashed lines in the upper illustration highlight the two kinds of Pr_3 triangles that abut each of the Pr centers. The lower drawing shows the overlap of hybrids from three adjacent trigonal prisms.

(11) Yee, K. A.; Hughbanks, T. *Inorg. Chem.* **1991**, *30*, 2321.
(12) Hulliger, F. *Structural Chemistry of Layer-type Phases*; Reidel: Dordrecht, The Netherlands, 1976.
(13) Warkentin, E. Dissertation, Universität Karlsruhe, 1977.

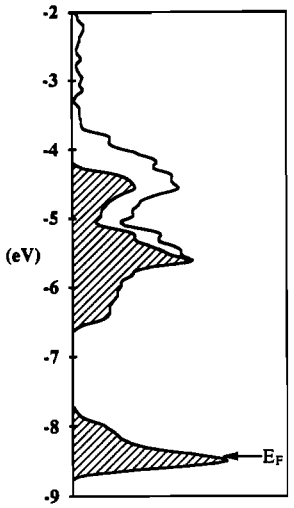

Figure 3. DOS (density of states) calculated for PrI_2, where levels in the Pr 5d band region are shown. The shaded parts indicate the bands from which both the valence and conduction band localized orbitals are constructed (see Figure 4). The Fermi level indicated is appropriate for a metallic ground state.

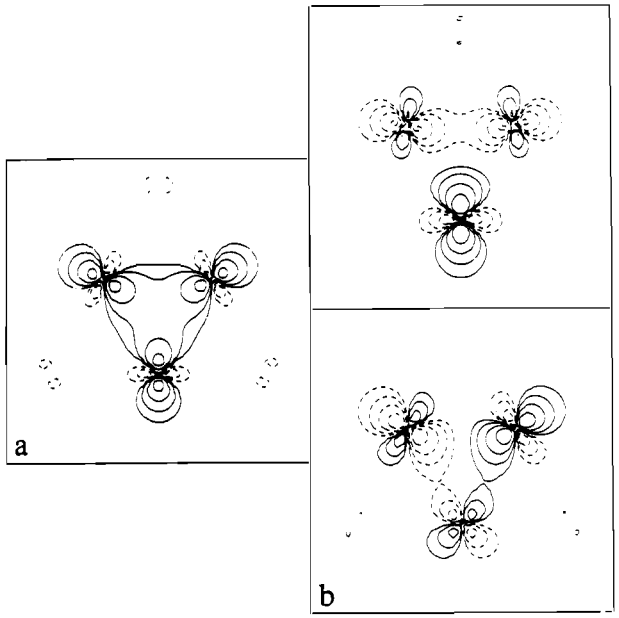

Figure 4. (a) Contour plot for the localized 3c-bonding orbital in the layer plane of PrI_2. The contours are ±0.4, ±0.2, ±0.1, and ±0.05. (b) Contour plots for two members of the e′ set of PrI_2. The contours are ±0.48, ±0.24, ±0.12, and ±0.06.

projected DOS indicates the bands from which the local orbitals are constructed. The extended Hückel method was used in all calculations. Local orbitals for the valence and conduction bands are plotted in Figure 4 and show just the character we have described. In order to demonstrate that our localization of the valence band Wannier orbitals in the uncapped Pr_3 is not due to an arbitrary decision on our part, Figure 5 shows the result of an attempt to construct a localized orbital that is centered in one of the *bicapped* triangles illustrated in Figure 2. This orbital is best understood as a linear combination of three adjacent local orbitals that are centered on neighboring *uncapped* Pr_3 triangles.

There are some energies that we can extract from this calculation that are of interest: the calculated band gap (E_g = 1.26 eV); the energy difference between the bottom of the valence and the top of the conduction bands (E_d = 4.30 eV); the widths of valence and conduction bands (E_v = 0.82 eV, E_c = 2.21 eV); the energy difference between the barycenters of the valence band and conduction band ($\Delta E(e' - a_1')$ = 2.95 eV). While higher-lying Pr 5d bands are pushed up by Pr–I antibonding interactions,

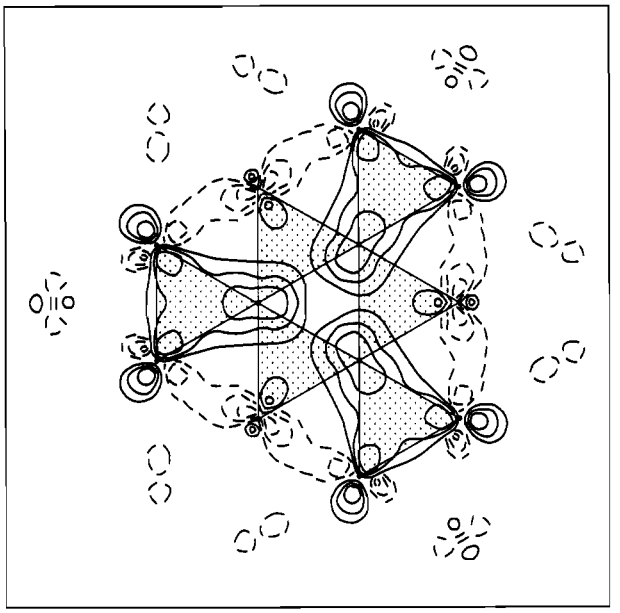

Figure 5. A contour plot in which an attempt was made to localize the valence band Wannier function in the bicapped Pr_3 triangles of layer structure depicted in Figure 2. The shaded triangles indicate the positioning of the *uncapped* Pr_3 triangles. Note the poor localization and the higher amplitude this orbital shows in the uncapped triangles. The contours are ±0.2, ±0.1, ±0.05, and ±0.025.

E_d is a measure of the 5d bandwidth that is largely due to Pr–Pr interactions. $\Delta E(e' - a_1')$ is a measure of the splitting between the bonding and antibonding orbitals of an "isolated" 3-center system (note that the labels here do *not* refer to the splitting between d_{z^2} and $\{d_{x^2-y^2}, d_{xy}\}$). Finally, E_v and E_c are respectively measures of the extent to which the otherwise noninteracting 3-center bond systems do indeed interact with each other. It is interesting that $\Delta E(e' - a_1')$ is about 69% of E_d, so that the splitting within the 3-center systems represents the major contribution to the bandwidth.

Factors Influencing the Valence Bandwidth

In PrI_2, we built up the key features of the electronic structures by use of three equivalent in-plane d orbitals that pass through the square faces of the three prism faces. If we consider an isolated trigonal prismatic center, and ignore the ligand contributions to the a_1' and e′ orbitals, these hybrids have an energy that is the weighted mean of the d_{z^2} and $\{d_{x^2-y^2}, d_{xy}\}$ orbitals from which they are constructed. There are finite matrix elements that couple them

$$\langle \sigma_1|H^{eff}|\sigma_1\rangle = \langle \sigma_2|H^{eff}|\sigma_2\rangle = \langle \sigma_3|H^{eff}|\sigma_3\rangle = 1/3(E_{a_1'} + 2E_{e'}) \quad (2)$$

$$\langle \sigma_1|H^{eff}|\sigma_2\rangle = \langle \sigma_1|H^{eff}|\sigma_3\rangle = \langle \sigma_2|H^{eff}|\sigma_3\rangle = 1/3\,(E_{a_1'} - E_{e'}) \quad (3)$$

where $E_{a_1'}$ and $E_{e'}$ are the energies of the a_1' and e′ orbitals. (Exactly analogous relations hold for sp^2 or sp^3 hybrids, if one wishes to build up the electronic structure of organic molecules or solids from a hybrid basis.[14]) One may easily verify that the original d-level splitting is recovered by solving the 3 × 3 secular determinant involving these hybrids. We can use these relations to get some insight into the origins of the valence band broadening by analyzing this question with the Wannier basis for the electronic structure in mind.

(14) Dewar, M. J. S. *Bull. Soc. Chim. Belg.* **1979**, *88*, 957.

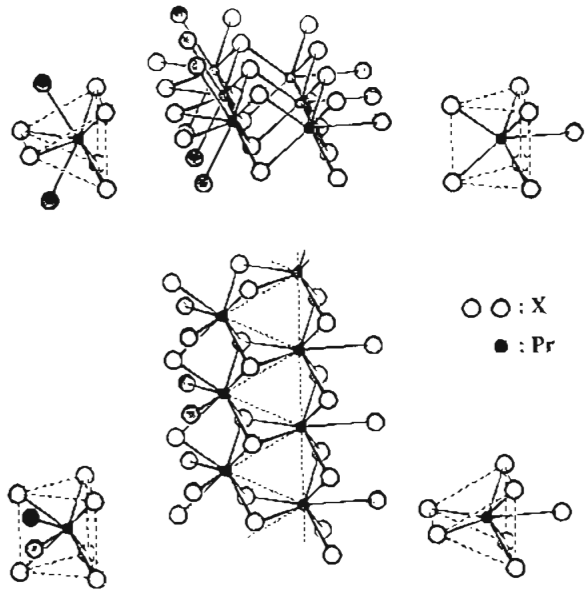

Figure 6. Double chains of monocapped and bicapped trigonal prisms in Pr_2X_5. The double chains are shown in perspectives differing by a 90° rotation. The monocapped and bicapped prisms are shown to guide the eye.

As the energy gap between the d_{z^2} and $\{d_{x^2-y^2},d_{xy}\}$ goes to zero, so does the interaction between the three hybrids. If we are near this point, then there are important implications for the valence band Wannier orbitals of the systems we have considered. As we have demonstrated, each of the Wannier orbitals is very well localized in each of the metal triangles of the structures discussed. This will be the case if metal–metal interactions are significantly larger than the splitting between the d_{z^2} and $\{d_{x^2-y^2},d_{xy}\}$ orbitals. Beyond that, to the extent that the Wannier orbitals are just combinations of hybrids on neighboring centers, the interaction between adjacent 3-center orbitals ($\omega(\mathbf{r})$ and $\omega(\mathbf{r}+\mathbf{a})$) can be estimated as due to the interaction between the hybrids on the single center that the three center bonds share:

$$\langle\omega(\mathbf{r})|H^{\text{eff}}|\omega(\mathbf{r}+\mathbf{a})\rangle \cong 1/3\langle\sigma_1|H^{\text{eff}}|\sigma_2\rangle = 1/9(E_{a_1'}-E_{e'}) \quad (4)$$

But this interaction between adjacent Wannier orbitals determines the width of the band from which they were constructed. Considering the band structure of these systems in the basis of the Wannier functions, we find that the interaction between the Wannier basis orbitals scales as the d_{z^2}–$\{d_{x^2-y^2},d_{xy}\}$ orbital splitting—as long as that splitting remains smaller than the metal–metal interaction. (As the quantity in (4) becomes very small, secondary interactions due to nonmetal contributions and next nearest neighbor overlaps will contribute.) The d_{z^2}–$\{d_{x^2-y^2},d_{xy}\}$ orbital splitting determines the valence bandwidth, not the gap between the valence and conduction band.

Pr_2X_5 (X = Br, I)

The Pr_2X_5 (X = Br, I) structures are considerably more complex but have been very nicely treated in recent papers to which we refer readers interested in details.[10,15] Meyer and Hoffmann have emphasized the important structural unit on which we shall focus,[10] the double chains depicted in Figure 6. The structural section shown consists of two chains of fused trigonal prisms. There are two kinds of prisms, monocapped and bicapped. Monocapped prisms are condensed into chains by fusion of two edges on the capped face with those of adjacent prisms (see the lower illustration in Figure 6; the chains to which we refer run vertically on the right-hand side). The bicapped prisms also form chains but via condensation of opposite trigonal faces (in the lower illustration in Figure 6, the chains run vertically on the left-hand side). Finally, these two chains are condensed together so that the prisms in one chain rotate by 90° with respect to the prisms in the other. Further condensation of this structural unit yields the full three-dimensional structure.[9,15]

(15) Schleid, T.; Meyer, G. *Z. Anorg. Allg. Chem.* **1987**, *552*, 97.

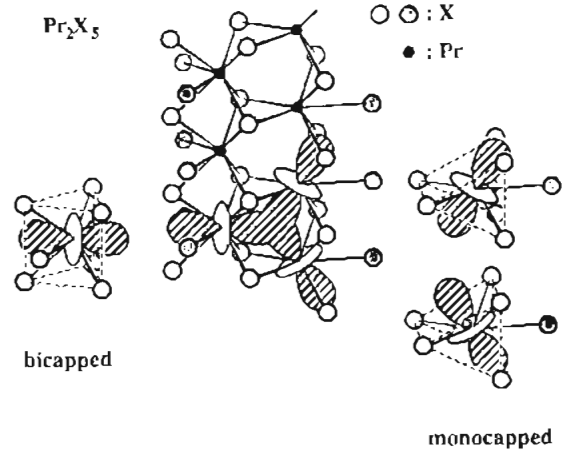

Figure 7. Assembly of the 3-center bonds for Pr_2X_5 structures from the hybrid orbitals of the constituent monocapped and bicapped prisms.

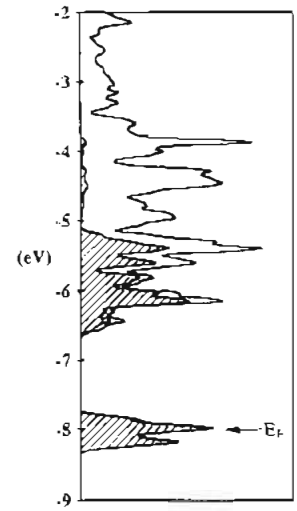

Figure 8. DOS (density of states) calculated for Pr_2Br_5, where levels in the Pr 5d band region are shown. The shaded parts are the 5d orbital combinations that correspond to the frontier hybrid orbitals depicted in Figure 7. The Fermi level indicated is appropriate for a metallic ground state.

Our electronic building blocks (2) allow us to understand the essentials of the electronic structure. Capping of a single prism face with a halide eliminates one hybrid from possible Pr–Pr bonding, since the hybrid directed into that face becomes involved in Pr–X bonding. Thus, each monocapped prism has two hybrids available for Pr–Pr bonding, while the bicapped prisms have one such hybrid. In both cases the hybrids are directed for bonding through the uncapped prism faces. Figure 7 shows the assembly of the 3-center bonds from these hybrids; each of the bicapped, eight-coordinate Pr centers participate in one 3-center bond, while the monocapped seven-coordinate Pr centers each participate in two adjacent 3-center bonds.

Figure 8 shows the DOS for Pr_2Br_5, calculated in a manner that exactly follows Meyer and Hoffmann except that no f orbitals were included in our calculation.[10] Included in this figure is a projection of the Pr orbital combinations corresponding to the frontier orbitals depicted schematically in Figure 7. Of course, the total DOS reported here is essentially indistinguishable from that reported earlier. We have taken the analysis only one step further and constructed the valence band Wannier orbitals for

this system, one of which is shown as a contour plot superimposed on the structure in **3**. We find that the 3-center bonding character

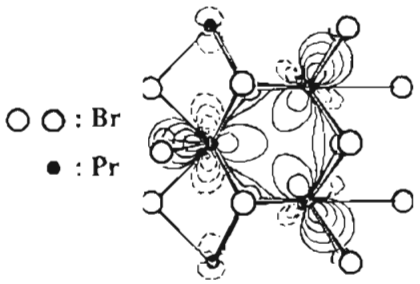

3

of this band comes out just as was rationalized in the above discussion and as suggested in Meyer and Hoffmann's treatment. (Actually, each unit cell contains two symmetry-related double chains like that shown in Figure 6, so there are two bands per Pr_4Br_{10} unit. The detailed band structure shows very small splittings of these bands, which is indicative of very weak interactions between these double chains. Two identical Wannier orbitals can be constructed, one for each chain.) The charge distribution in the valence band is apparent in the Wannier orbital plot in **3**, and Mulliken population analysis shows an almost exact 2:1 partitioning of charge density for the valence band between the seven- and eight-coordinate Pr centers.

Other features of these systems indicate a close analogy with the PrI_2 system. The valence-conduction band gaps (E_g) for Pr_2Br_5 and Pr_2I_5 are calculated to be 1.23 and 0.77 eV, respectively. The projected DOS in Figure 8 shows a pattern clearly reminiscent of the PrI_2 system, and Wannier orbitals for conduction bands of Pr_2Br_5 closely resemble the conduction band local orbitals depicted for PrI_2 in Figure 4b. Using plots for Pr_2Br_5 and Pr_2I_5, we obtain the following numerical results: for Pr_2Br_5, $E_v = 0.47$ eV, $E_c = 1.38$ eV, $\Delta E(e' - a_1') = 2.29$ eV; for Pr_2I_5, $E_v = 0.47$ eV, $E_c = 1.83$ eV, $\Delta E(e' - a_1') = 2.06$ eV. The valence bandwidth is unchanged on moving from Pr_2Br_5 to Pr_2I_5, despite an increase in the Pr–Pr distances (Pr_2Br_5, 4.166 and 4.210 Å; Pr_2I_5, 4.32 and 4.52 Å).[9] The values of E_g and $\Delta_E(e' - a_1')$, which depend on the 3c-bond orbital splitting, both decline as the Pr–Pr distances increase.

Properties: Potential and Actual Electronic Localization

What are the properties of these compounds? All of the metals of concern here are trivalent, a tendency that is empirically well correlated with the elements' standard reduction potentials[16,17] and consistent with the measured Ln–X bond lengths.[9,15] Of the diiodides, only for LaI_2 have resistivity measurements been reported.[18] GdI_2 exhibits strongly coupled ferromagnetic layers of Gd^{2+} moments ($T_C = 313$ K) and has been described as a very good approximation of a two-dimensional Heisenberg system.[19] It has been generally assumed that the compound is metallic, and as in the ferromagnetic bulk Gd metal ($T_C = 293$ K), RKKY interactions mediated by the conduction electrons are responsible for coupling the ionic ^8S cores.[19-22] But there are no reported resistivity data that support this supposition. Detailed studies show both of the Pr_2X_5 (X = Br, I) systems to be semiconductors with room-temperature bulk resistivities greater than 10^3 Ω-cm, and both have high antiferromagnetic ordering temperatures (Pr_2Br_5, $T_N = 50$ (1) K; Pr_2I_5, $T_N = 37$ (1) K).[9] Still, the Pr^{3+} ions in each compound have the f^2 core configurations typical of trivalent ions.

Clearly, mathematically constructing local orbitals for the valence bands of compounds like PrI_2 and Pr_2Br_5 is not sufficient to show that the electrons in these half-filled band cases will localize. The energetic price the system must pay for localization consists of "mixing in" crystal orbital character from the otherwise unoccupied band orbitals and is therefore proportional to the bandwidth, W. To the extent that this mixing is confined to the valence band, our Wannier orbitals give a good representation of the "location" of the localized electrons. In fact, the available evidence indicates that electrons do localize in both of the Pr_2X_5 compounds but are not localized in LaI_2. Our treatment of these systems indicates that the line which divides these compounds must be a fine one. The calculated bandwidth for PrI_2 is only moderately larger than that for Pr_2I_5 (0.82 vs 0.47 eV). As we have seen, the character of the valence band in each is very similar.

The similarity in the electronic structure of both classes of compound strongly indicates that metallic behavior should not be assumed for any of the aforementioned diiodides for which resistivity data have not actually been measured. While the metallic character of LaI_2 argues for the same character of GdI_2, the magnetic, localized, ground state of Pr_2I_5 indicates otherwise. The strong magnetic coupling in GdI_2 need not involve RKKY coupling, but might be correlated with a magnetically ordered 5d subsystem, as occurs in the Pr_2X_5 compounds.

We conclude with some comments on the chemical analogies that exist between the group V disulfides, $(Nb,Ta)S_2$, and the LnI_2 compounds discussed. The electronic similarities are now quite clear: each of these systems has a d^1 configuration and a set of 3-center bond orbitals that are half-occupied. The question of electron localization aside, there exists the obvious possibility that the halides discussed here may exhibit a hydrogenation chemistry like the $(Nb,Ta)S_2$ compounds, for which $H_x(Nb,Ta)S_2$ can be synthesized.[23] In these compounds, hydrogen was shown to sit at the center of the uncapped M_3 triangle.[24] This was discussed in our previous paper, but in essence the bonding involves the formation of a bonding electron pair by interaction of a half-occupied 3-center M_3 system with a hydrogen atom.[11] Clearly, the same should be possible for the systems discussed above, as has been demonstrated by Meyer and Hoffmann for $H(Pr_2Br_5)$.[10] We note that this chemistry may have already been demonstrated by Struss and Corbett, though without structural characterization of the products. These investigators have shown that many of the trivalent dihalides take up hydrogen at 400 °C in amounts suggesting possible incorporation into the Ln_3 triangles we have discussed.[25] Hydrogenation of LaI_2 at higher temperatures seems to lead to products that do not adopt a MoS_2-type structure.[26] Finally, we note that, in the synthesis of reduced rare earth compounds, the reducing agent is usually the elemental metals. The presence of adventitious hydrogen from this source (or others) is often a potential problem—those who study the properties of LnX_2 compounds will have to be especially careful that their measurements do not actually apply to materials that are stabilized by interstitial hydrogen.

Summary

We emphasize that the localization of 5d electrons as discussed herein is not a result of narrow d bands that arise because

(16) Morss, L. R. *Chem. Rev.* **1976**, *76*, 827.
(17) Johnson, D. A. *Some Thermodynamic Aspects of Inorganic Chemistry*; 2nd ed.; Cambridge University Press: Cambridge, U.K., 1982.
(18) Corbett, J. D.; Sallach, R. A.; Lokken, D. A. *Adv. Chem. Ser.* **1967**, *No. 71*, 56.
(19) Kasten, A.; Müller, P. H.; Schienle, M. *Solid State Commun.* **1984**, *51*, 919.
(20) Mee, J. E.; Corbett, J. D. *Inorg. Chem.* **1965**, *4*, 88.
(21) Mattis, D. C. *The Theory of Magnetism I*; Springer-Verlag: New York, 1981.
(22) White, R. M. *Quantum Theory of Magnetism*; 2nd ed.; Springer-Verlag: New York, 1983.
(23) Murphy, D. W.; Disalvo, F. J.; Hull, G. W. J.; Waszczak, J. V.; Mayer, S. F.; Stewart, G. R.; Early, S.; Acrivos, J. V.; Geballe, T. H. *J. Chem. Phys.* **1975**, *62*, 967.
(24) Rickel, C.; Reznik, H. G.; Schöllhorn, R.; Wright, C. J. *J. Chem. Phys.* **1979**, *70*, 5203.
(25) Struss, A. W.; Corbett, J. D. *Inorg. Chem.* **1978**, *17*, 965.
(26) Imoto, H.; Corbett, J. D. *Inorg. Chem.* **1981**, *20*, 630.

Table I. Parameters for EH Calculations

	orbital	H_{ii}, eV	ζ_1[b]	ζ_2[b]	c_1[a]	c_2[a]
Pr	5d	−8.08	2.75	1.267	.7187	.4449
	6s	−7.42	1.40			
	6p	−4.65	1.40			
Br	4s	−28.0	2.64			
	4p	−13.9	2.26			
I	5s	−24.5	2.68			
	5p	−13.0	2.32			

[a] Coefficients used in double-ζ expansion. [b] Slater-type orbital exponents.

interaction among the metal centers is weak. Rather, the localization arises because of specific structural characteristics of the materials discussed and the orbital localization that is possible for these structures. While the direct metal–metal bonding *is* modest in these compounds, the d band splittings induced by metal–metal bonding are sufficient to open up significant energy gaps between valence and conduction bands. Certainly then, our treatment indicates that the long metal–metal distances in these compounds have no direct bearing on the issue of 5d electron localization. The narrow width of the partially occupied valence bands occurs because of the weak coupling between multicenter bond orbitals. An intricate balance is struck that determines whether compounds like Pr_2X_5 (X = Br, I), GdI_2, or either of the trigonal prismatic modifications of PrI_2 are metallic or insulating. This balance is between the electronic repulsion that tends to localize 5d electrons into individual multicenter bond orbitals and the width of the band from which the multicenter bond orbitals arise. In the language of a Hubbard model, the electronic repulsion is identified with the parameter U and the bandwidth is W.[21,22]

Perhaps the most interesting aspect of these problems is the fact that neither U nor W has the physical origin that is conventionally assumed. The electronic repulsion U is generally thought to be some sort of *on-site* interaction. Our treatment shows that if we adopt that view in these compounds, the "site" must be understood to have a rather delocalized multicenter character. This provides at least a partial explanation of why U is much smaller than we would expect if it represented an intraatomic repulsion term; the delocalization of the Wannier functions should lead to decreased electron repulsion. The bandwidth W is generally assumed to be proportional to the orbital interaction between metal centers (an interatomic resonance integral). Our treatment shows that the valence bandwidth is better understood as proportional to the interaction between multicenter bonds, which turns out to vary with c/a for the trigonal prismatic building blocks.

Acknowledgment. We gratefully acknowledge the National Science Foundation for its support through a Presidential Young Investigator Award (Grant DMR-8858151) and the Robert A. Welch Foundation for its support through Grant A-1132.

Appendix

All calculations employed the extended Hückel (tight-binding) method;[27,28] parameters appear in Table I. Exponents for the halides came from Clementi and Roetti;[29] parameters for Pr were taken from Meyer and Hoffmann.[10,30] The DOS curve in Figure 3 entailed the use of 91 k-points in the irreducible wedge of the two-dimensional hexagonal Brillouin zone. For Pr_2Br_5 (Figure 8), a 108 k-point mesh covered half of the zone.

Wannier functions were constructed by following the prescription outlined in previous papers.[7,11] In all cases, the number of k points (N_k) in the entire first Brillouin zone for the band structure calculations must be large enough that the extent of localization of the Wannier functions is unaffected by increasing N_k. In practice this means that the Wannier function must be well localized within a radius, $r_0 \approx (a/2)(N_k)^{1/n}$, where a is a typical lattice parameter for the system and n is the dimensionality of the system (n = 1, 2, or 3). For the calculation of Wannier functions for Pr_2Br_5 we found it convenient to double the size of the unit cell so that entire Pr_3 triangles were contained within it. With this expanded cell, we performed a calculation using 108 k points in half of the three-dimensional Brillouin zone. The other half of the zone simply yields complex conjugate wave functions which need not be calculated; for the purposes of estimating r_0 in the above formula, N_k = 216. Local orbital construction for PrI_2 exactly followed that for MoS_2.[11] The dissimilarity in the conduction band local orbitals for MoS_2 and PrI_2 is due to numerical errors made in our previous work; the correct conduction band local orbitals for MoS_2 bear a closer resemblance to those shown for PrI_2 (Figure 4b).

(27) Whangbo, M.-H.; Evain, M.; Hughbanks, T.; Kertesz, M.; Wijeyesekera, S.; Wilker, C.; Zheng, C.; Hoffmann, R. *QCPE* **1989**, *9*, 61.
(28) Hoffmann, R. *J. Chem. Phys.* **1963**, *39*, 1397.
(29) Clementi, E.; Roetti, C. *At. Nucl. Data Tables* **1974**, *14*, 177.
(30) Ortiz, J. V.; Hoffmann, R. *Inorg. Chem.* **1985**, *24*, 2095.